Journal of Colloid and Interface Science **215,** 381–396 (1999)
Article ID jcis.1999.6258, available online at http://www.idealibrary.com on IDEAL®

Hydrodynamic Instability of Liquid Films on Moving Fibers

Konstantin G. Kornev* and Alexander V. Neimark†,[1]

**Institute for Problems in Mechanics, Russian Academy of Sciences, Prospect Vernadskogo 101, Moscow 117526, Russia; and †TRI/Princeton, 601 Prospect Avenue, Princeton, New Jersey 08542-0625*

kornev@ipmnet.ru, aneimark@triprinceton.org

Received December 14, 1998; accepted March 30, 1999

The stability of liquid films on moving fibers is studied with a focus on effects caused by film–solid adhesion interactions and hydrodynamic interactions between the film and the surrounding gas. We show that at high fiber velocities (large Reynolds numbers) the film–gas hydrodynamic interactions induce instability in films, which would, otherwise, be stabilized by the adhesion interactions at static conditions. Two types of unstable modes caused by hydrodynamic factors are found: the first corresponds to the Kelvin–Helmholtz waves induced by inertia effects; the second, induced by viscosity effects, is observed at smaller (yet still large) Reynolds numbers when the Kelvin–Helmholtz instability is suppressed. Linear stability analysis of the system of coupled hydrodynamic equations of film and gas flow is performed by the method of normal modes. We derive the general dispersion relation as an implicit equation with respect to the mode frequency. In the limit of vanishing fiber velocities, the obtained equation provides the dispersion equation for motionless fibers. The conditions of film stability and unstable modes are analyzed in terms of two dimensionless parameters, the adhesion factor, which quantifies the intensity of film–fiber interactions, and the Weber number, which quantifies the intensity of film–gas interactions. The Reynolds number determines the regions of validity of the inviscid and viscous regimes of film instability. The results are illustrated by estimates of the stability conditions for moving fibers in terms of the stability diagram, the critical film thickness, the fastest unstable mode, and the corresponding characteristic break-up time. Although the methods developed are applicable for any type of liquid–solid interaction, the estimates were made for the long-range van der Waals interactions. Practical applications include various technologies related to fabrication and chemical modifications of fibers and fiber products, e.g., spin finishing and lubrication.

Key Words: **liquid films; fibers; hydrodynamic instability; adhesion.**

I. INTRODUCTION

The problem of stability of thin liquid films on cylindrical solid surfaces has been drawing permanent attention of researchers on account of many important practical applications, including coating of fibers and wires, spin finishing, chemical modification, and drying of textiles and other fibrous materials. It is well documented in the literature that wetting properties of curved substrates may differ significantly from those of plane surfaces (1–15). Specific curvature-dependent effects come from the competition between the capillarity and long-range intermolecular forces. Much work has been done to explore the conditions of film stability on *motionless* fibers (6–8, 10–12, 16–26).

Convex surfaces of fibers[2] imply positive curvatures of coating liquid films and, therefore, a positive Laplace pressure acting on the outer film interface:

$$P_c = p_l^0 - p_g^0 = \frac{\gamma}{R_f + h}. \qquad [1]$$

Here, γ is the liquid–gas surface tension, R_f is the fiber radius, p_i^0 are pressures in the gas, $i = g$, and liquid, $i = l$, phases, and h is the film thickness. Laplace pressure, when positive, tends to squeeze the liquid out of the film. This effect causes a well-known phenomenon of capillarity-driven instability of films coating cylindrical solid surfaces, similar to the Rayleigh instability of jets (27). Goren (16), and then other researchers (Johnson *et al.* (23), Yarin *et al.* (25)), studied in detail the Rayleigh instability of liquid films on cylindrical fibers without taking into consideration liquid–solid interactions, or, in other words, adhesion. They concluded that the uniform liquid coating is always unstable and collapses into a periodic array of droplets, independent of film thickness, fiber radius, and liquid properties, such as viscosity, surface tension, and density. The above-mentioned physical parameters determine the rate of film destruction.

Adhesion between liquid and solid may stabilize the films. Thermodynamic equilibrium and stability of thin films on curved solid surfaces are determined by competition between capillarity and adhesion forces. While the curvature-dependent Laplace pressure favors the liquid spreading over the solid surface, the thickness-dependent film–solid interactions oppose

[1] To whom correspondence should be addressed. Fax: 609 683 7149.

[2] Below, we use the term "fiber" for any cylindrical solid substrate (fibers, wires, threads, etc.).

0021-9797/99 $30.00

the film thinning. An equilibrium liquid configuration is observed when these forces are in balance. Derjaguin (28, 29) developed a concept of disjoining pressure, which is currently regarded as the most practical rationale to account for film–solid interactions (1–3). In the so-called Derjaguin approximation (1–3), it is assumed that the disjoining pressure, $\Pi(h)$, depends exclusively upon the film thickness and is additive to the Laplace pressure. In particular, for a uniform film of thickness h_0 on a cylindrical fiber the pressure difference across the film–gas interface is represented as a sum of the Laplace pressure [1] and the disjoining pressures, $\Pi(h_0)$:

$$-\frac{\gamma}{R_f + h} + \Pi(h_0) = p_g^0 - p_l^0 = -P_c. \qquad [2]$$

Starov and Churaev (6) discussed the curvature-dependent effects in terms of Eq. [2] for model isotherms of disjoining pressure. In most practical systems, the behavior of thin films is mainly determined by long-range dispersion, or van der Waals forces. Brochard-Wyart (7, 8) has shown that liquid films on fibers can be stabilized due to the action of dispersion forces. She analyzed conditions of thermodynamic equilibrium and derived a stability criterion for the van der Waals films on fibers. The role of dispersion interactions has been studied by Nowakowski and Ruckenstein (13), with respect to the spreading of small droplets, and recently by Chen and Hwang (26), who rendered a nonlinear analysis of film stability in the lubrication approximation.

Effects of short-range interactions (acid–base, hydrophobic, etc.) have been recently studied by Neimark (30) with applications to equilibrium configurations of liquid droplets and contact angles on fibers. A new equation for contact angles on cylindrical fibers has been derived to account for the fiber curvature and the liquid–solid interactions expressed in terms of the disjoining pressure isotherm.

In this paper, we analyze the stability of liquid films on *moving* fibers that requires a better understanding of specific interactions among film, fiber, and flowing air. This problem has important practical applications to spin finishing and fiber coating technologies, in which fiber velocities may exceed 100 km/h (31). We show that hydrodynamic interactions between the coating film and the surrounding air cause an additional source of instability, responsible for film destruction, droplet formation, and slinging.[3] To the best of our knowledge, this effect, which we have named the *wind effect*, has not been considered in the literature so far. We develop a general theory of the stability of films on moving fibers for different types of fluid–solid interactions, and formulate conditions of thermodynamic and hydrodynamic equilibrium. Stability diagrams and asymptotic estimates are derived for different adhesion and hydrodynamic regimes.

[3] The term "slinging" is used in the fiber industry to describe the droplet break-away from the moving fibers.

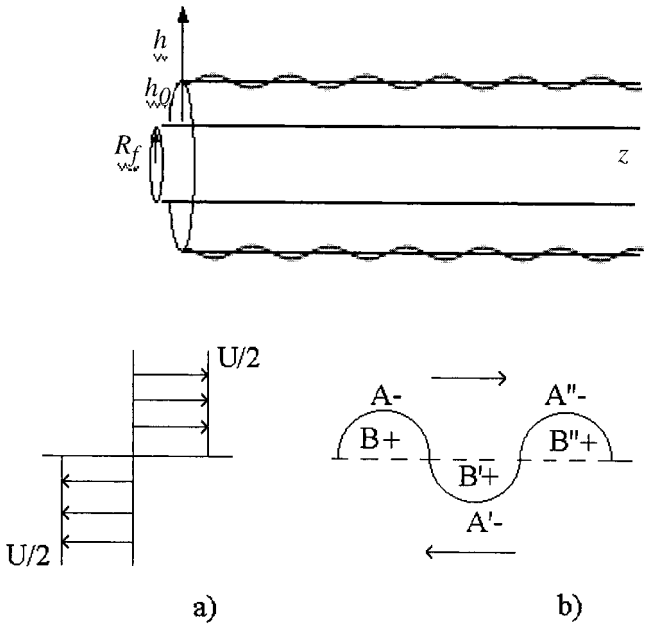

FIG. 1. Disturbances of film surface and schematic explanation of the Kelvin–Helmholtz mechanism of film instability.

II. THERMODYNAMIC STABILITY OF LIQUID FILMS ON FIBERS

Let's first discuss conditions of thermodynamic stability of films on motionless fibers. Laplace pressure across a curved interface depends on two principal radii of curvature,

$$P_L = \gamma\left(\frac{1}{R_1} + \frac{1}{R_2}\right). \qquad [3]$$

For a uniform film on a cylindrical fiber, $R_1 = \infty$, $R_2 = R_f + h$, and Eq. [3] reduces to Eq. [1]. Consider the perturbation $h = h_0 + \zeta(z, t)$ of a gas–liquid interface; here h_0 is the thickness of the undisturbed uniform film (Fig. 1). A disturbance of the liquid–gas surface causes local changes in the capillary pressure. Using general differential forms for the principal radii of curvature, the Laplace pressure is expressed through the second and first derivatives of surface displacement (32–34):

$$P_L = \gamma\left[-\frac{\zeta''}{(1+\zeta'^2)^{3/2}} + \frac{1}{(R_f + h_0 + \zeta)(1+\zeta'^2)^{1/2}}\right] \approx \frac{\gamma}{R_f + h_0} - \gamma\left[\zeta'' + \frac{\zeta}{(R_f + h_0)^2}\right]. \qquad [4]$$

To suppress the interface disturbances, the upward (positive ζ) surface displacements have to cause a local increase, and correspondingly, the downward (negative ζ) displacements have to cause a local decrease in the liquid pressure. In other

words, to ensure stability, the liquid pressure disturbances, represented by the second term in the RHS of Eq. [4], must have the same sign as the surface disturbances,

$$\zeta\left[\zeta'' + \frac{\zeta}{(R_f + h_0)^2}\right] < 0. \quad [5]$$

For harmonic perturbations, $\zeta = A \cos kz$ (Fig. 1), the stability condition [5] reads as

$$\left(-k^2 + \frac{1}{(R_f + h_0)^2}\right) < 0. \quad [6]$$

Inequality [6] is the classical Plateau criterion of jet stability (32).

For thin films, Eq. [3] is modified by the disjoining pressure, $\Pi(h)$, which acts in a film in addition to the capillary pressure (1–3),

$$P_l - P_g = \gamma\left(\frac{1}{R_1} + \frac{1}{R_2}\right) - \Pi(h). \quad [7]$$

For an undisturbed uniform film, Eq. [7] reduces to Eq. [2]. For a disturbed film, the liquid pressure disturbance depends on variations of the film curvature and of the film thickness,

$$\delta P = -\gamma\left[\zeta'' + \frac{\zeta}{(R_f + h_0)^2}\right] - \zeta\left.\frac{\partial \Pi(h)}{\partial h}\right|_{h=h_0}. \quad [8]$$

Correspondingly, the stability criterion, inequality [6], written for the wave numbers, is modified as

$$-k^2(R_f + h_0)^2 + 1 + \frac{(R_f + h_0)^2}{\gamma}\left.\frac{\partial \Pi}{\partial h}\right|_{h=h_0} = -k^2(R_f + h_0)^2 + \Delta < 0. \quad [9]$$

Here, *the thermodynamic stability factor*,

$$\Delta = 1 + \frac{(R_f + h_0)^2}{\gamma}\Pi'(h_0), \quad [10]$$

is introduced. The modes are leveled out if condition [9] is fulfilled. Thus, the adhesion expands the range of admissible perturbations. Moreover, when the thermodynamic factor Δ is negative, any infinitesimal disturbance is suppressed due to the action of the fluid–solid interactions independent of the wavelength (7).

For thick films, the dispersion forces are dominant in film–substrate coupling. The dispersion component of the disjoining pressure is $\Pi(h) = a_{HL}^2\gamma/h^3$ (7); the constant a_{HL} is the modified Hamaker–Lifshitz constant, $a_{HL} \propto O$ (Å) (3, 8). From the criterion of thermodynamic stability, [9] and [10], it follows that the films of thickness $h_0 < h_c = 3^{1/4}\sqrt{a_{HL}R_f}$ are stable (7). An estimate gives $h_c \approx 0.1$ μm for fibers of $R_f = 100$ μm. Films of thickness $h_0 > h_c$ are unstable with respect to disturbances of wavelength, $\lambda = 2\pi/k > 2\pi(R_f + h_0)/\sqrt{\Delta} \approx 2\pi R_f/\sqrt{1 - (h_c/h)^4}$ (7).

The above analysis concerns the motionless fiber. If the fiber is moving, hydrodynamic interactions between the film and the surrounding gas cause interfacial disturbances, which may lead to destruction of thermodynamically stable films.

III. HYDRODYNAMIC STABILITY: THE PROBLEM FORMULATION

Consider a fiber moving with velocity $-U$ in the z direction. For fiber coating applications such as spin finishing the following data are typical: $R_f = 10$ μm, $U = 10^4$ cm/s (31). Then, the Reynolds number for air $\mathrm{Re}_g = UR_f\rho_g/\eta_g$ is large, on the order of 10^2 ($\rho_g \approx 10^{-3}$ g/cm^3 is the gas density and $\eta_g \approx 10^{-4}$ ps is the gas viscosity), so that the gas can be considered inviscid. The hypothesis of negligible air friction is also supported by the kinetic reasons. Since the free path length in the air at the atmospheric pressure is on order of 0.1 μm, the thermal excitations should wash out the boundary layer whose characteristic size l is estimated as $l \approx R_f/\sqrt{UR_f\rho_g/\eta_g} \approx 1$ μm (34).

Under these flow conditions, the characteristic time $1/\omega$ of growth of a wave with a length comparable with the fiber radius is much smaller than the diffusion time of propagation of associated vortices in the film. Therefore, the strong inequality $\eta_l/\rho_l \ll \omega/k^2$ takes place, where ρ_l is the fluid density and η_l is the fluid viscosity. For example, for water solutions/suspensions on typical textile fibers, $k \approx 1/R_f \approx 10^3$ cm^{-1}, $\omega \approx U/R_f \approx 10^4/10^{-3}$ s^{-1}, $\eta_l = 10^{-2}$ ps, $\rho_l \approx 10^3$ ρ_g, and we have got $\omega/k^2 \approx 10^7/10^6 = 10 \gg \eta_l/\rho_l \approx 10^{-2}$ cm^2/s. If the wavelength is smaller, $k \approx 1/h_0$, both times are comparable. Thus, when the Reynolds number for a liquid film $\mathrm{Re}_l = Uh_0\rho_l/\eta_l$ is large, the viscous terms in the Navier–Stokes equations may be neglected, so that both fluids, liquid and gas, can be considered inviscid. For the above-mentioned parameters, the range of film thicknesses acceptable for the purely inviscid model is estimated as $\mathrm{Re}_l = Uh_0\rho_l/\eta_l = (h_0/R_f)(UR_f\rho_l/\eta_l) \approx 10^3\,(h_0/R_f) \gg 1$. When the film is so thin that this strong inequality does not hold, the viscous effects in the film must be considered. However, the gas flow can be always treated in the inviscid approximation independent of the film thickness.

In case of inviscid fluids, we deal with a so-called Kelvin–Helmholtz mechanism of interfacial instability (Drazin and Reid (33), Landau and Lifshitz (34)). The Kelvin–Helmholtz mechanism is caused by inertia and is not related to interfacial tension and ratio of densities. The Kelvin–Helmholtz instability is schematically illustrated in Fig. 1, where the reference

frame is chosen as moving with velocity $U/2$ along the fiber, so that the phases are moving with equal velocities, $U/2$, in opposite directions. In case of harmonic perturbations of the interface, the fluid is accelerated at the convex regions of the deformed interface, points A, A′, and A″, and decelerated at the concave regions, points B, B′, and B″. In accordance with the Bernoulli equation, the smaller the speed, the greater the pressure. Thus, perturbations of the interface cause changes in velocity that in turn induces changes in pressure. The resulting pressure differences across the interface are directed so that they tend to amplify the initial disturbances.

Consider the instability mechanism in films on fibers in more detail *without using the inviscid approximation* for the liquid film flow in the initial equations. In the reference frame attached to the moving fiber the basic undisturbed flow is as follows. In the region of film $R_f < r < R_f + h_0$ (h_0 is the film thickness in the unperturbed state), the *viscous fluid* of density $\rho_l > \rho_g$ remains at rest. In the region $r > R_f + h_0$, the *inviscid gas* moves with a uniform velocity U in the $\bar{z}$ direction. Gravity is neglected. Then the system of equations for the flow perturbations takes the following form.

Equations for the Film Fluid

The film fluid is considered as incompressible and satisfies the equation of continuity

$$\nabla \cdot \boldsymbol{\nu}^l = 0. \tag{11}$$

We restrict ourselves to the initial stage of instability evolution, and therefore the linearized Navier–Stokes equations may be used for description of the flow pattern within the film,

$$\rho_l \frac{\partial \boldsymbol{\nu}^l}{\partial t} = -\nabla p_l + \eta_l \Delta \boldsymbol{\nu}^l. \tag{12}$$

Using the formula from vector analysis, $\nabla \cdot \nabla \boldsymbol{\nu} = \nabla(\nabla \cdot \boldsymbol{\nu}) - curl(curl\boldsymbol{\nu})$ (34), and accounting for the incompressibility condition [11], we can represent the velocity field as a sum of an irrotational velocity field and a rotational one, $\boldsymbol{\nu}^l = \mathbf{u}^l + \mathbf{V}^l$. The irrotational velocity field admits treatment in terms of a potential φ_l with $\mathbf{u}^l = \nabla\varphi_l$. The rotational components of the velocity field obey the incompressibility condition [11] and the following equations (34):

$$\rho_l \frac{\partial V_r^l}{\partial t} = \eta_l \left(\Delta V_r^l - \frac{V_r^l}{r^2} \right), \tag{13}$$

$$\rho_l \frac{\partial V_z^l}{\partial t} = \eta_l \Delta V_z^l. \tag{14}$$

The suggested subdivision of the velocity field allows us to treat the flow pattern as caused separately by inertial and viscous forces. No-slip at the solid boundary of the liquid annulus, $r = R_f$, gives

$$\frac{\partial \varphi_l}{\partial z} + V_z^l = 0, \tag{15}$$

$$\frac{\partial \varphi_l}{\partial r} + V_r^l = 0. \tag{16}$$

Equations for the Surrounding Gas

Because of a high velocity regime of gas flow, the gas compressibility may be appreciable. So, we write the continuity equation for air in a general form (34),

$$\frac{\partial \bar{\rho}_g}{\partial t} + \nabla \cdot (\boldsymbol{\nu}^g \bar{\rho}_g) = 0. \tag{17}$$

Subdividing the pressure and air density into the background values and perturbations as $p_g = \rho_g U^2/2 + p$, $\bar{\rho}_g = \rho_g + \rho$, we can use for perturbations the equation of state (34)

$$p = c^2 \rho, \tag{18}$$

where c is the sound velocity. Substituting Eq. [18] into Eq. [17], we obtain after linearization

$$\frac{\partial p}{\partial t} + c^2 \rho_g \nabla \cdot \boldsymbol{\nu}^g = 0. \tag{19}$$

Substituting in Eq. [19] the characteristic scale for pressure perturbations, $\rho_g U^2/2$, the characteristic time, R_f/U, and the characteristic scale for velocity gradients, U/R_f, we conclude that the compressibility effect is important when the asymptotic equation $U^2/c^2 \approx O(1)$ holds. Using for an estimate $U = 10^4$ cm/s and $c = 3.5 \times 10^4$ cm/s, we find the value $U^2/c^2 \approx 10^{-1}$. Thus, we still may treat the gas as incompressible, but the safety factor is small. Below, we use the continuity equation in the form

$$\nabla \cdot \boldsymbol{\nu}^g = 0. \tag{20}$$

Because of large Reynolds numbers, we may model the flow of air as the flow of an inviscid fluid. The velocity field $\boldsymbol{\nu}^g = \mathbf{U} + \mathbf{w}^g$ obeys Euler's equations,

$$\frac{\partial \boldsymbol{\nu}^g}{\partial t} + \boldsymbol{\nu}^g \cdot \nabla \boldsymbol{\nu}^g = -\frac{1}{\bar{\rho}_g} \nabla p_g, \tag{21}$$

and the boundary condition at infinity; namely, the perturbation of gas velocity must vanish at infinity,

$$|\mathbf{w}^g| \to 0, \quad \text{as } r \to \infty. \tag{22}$$

We also assume that the initially disturbed flow is irrotational and suppose the velocity potential φ_g with $\boldsymbol{\nu}^g = \mathbf{U} + \nabla\varphi_g$ to exist. Then, the incompressibility condition [20] is reduced to the Laplace equation for the velocity potential. Thus, both gas and liquid velocity potentials φ_i, $i = l, g$ obey the Laplace equation (we suppose that the motion is axially symmetric, i.e., that all the derivatives with respect to angle theta, in cylindrical coordinates, are zeros):

$$\frac{1}{r}\frac{\partial}{\partial r}\left(r\frac{\partial\varphi_i}{\partial r}\right) + \frac{1}{r^2}\frac{\partial^2\varphi_i}{\partial\theta^2} + \frac{\partial^2\varphi_i}{\partial\breve{z}^2} = 0. \qquad [23]$$

Coupling at the Film–Gas Interface

Since the viscosity ratio η_g/η_l is a small parameter, we can ignore the shearing action of air,

$$\left(\frac{\partial\nu_r^l}{\partial z} + \frac{\partial\nu_z^l}{\partial r}\right) = \frac{\eta_g}{\eta_l}\left(\frac{\partial\nu_r^g}{\partial z} + \frac{\partial\nu_z^g}{\partial r}\right) \ll 1. \qquad [24]$$

Despite the seemingly kindred statement for ordinary flows of inviscid fluids, both parts of the velocity field $\boldsymbol{\nu}^l$ are connected by the boundary conditions at the interface and fiber surface. We ascribe all variations of the pressure field to those caused by the irrotational component of the velocity field. Hence, the pressure can be obtained by using Bernoulli's theorem as

$$\rho_l\left(\frac{\partial\varphi_l}{\partial t}\right) + p_l = 0. \qquad [25]$$

Similarly, linearization of Bernoulli's equation by neglecting products of the increments gives the gas pressure at the interface as

$$\rho_g\left(\frac{\partial\varphi_g}{\partial t} + U\frac{\partial\varphi_g}{\partial\breve{z}}\right) + p_g = 0. \qquad [26]$$

The kinematic condition that each surface particle remains on the surface gives

$$\frac{\partial\zeta}{\partial t} + U\frac{\partial\zeta}{\partial\breve{z}} = \frac{\partial\varphi_g}{\partial r}, \qquad [27]$$

$$\frac{\partial\zeta}{\partial t} = \frac{\partial\varphi_l}{\partial r} + V_r^l. \qquad [28]$$

Since the tangential stress at the free surface of liquid is zero, Eq. [24], we have

$$2\frac{\partial^2\varphi_l}{\partial z\partial r} + \frac{\partial V_r^l}{\partial z} + \frac{\partial V_z^l}{\partial r} = 0. \qquad [29]$$

We also have to take into account that the normal component of the stress tensor jumps by the Laplace and disjoining pressures at the interface, $r = r_0 = R_f + h_0$,

$$p_g - \gamma\left(\frac{\zeta}{r_0^2} + \frac{\partial^2\zeta}{\partial z^2}\right) = \left.\frac{\partial\Pi}{\partial h}\right|_{h=h_0}\zeta + p_l - 2\eta_l\frac{\partial V_r^l}{\partial r}. \qquad [30]$$

Thus, the hydrodynamic model for stability analysis consists of the closed system of linear equations [11], [13], [14], [23] subjected to the boundary conditions [22], [24]–[30].

IV. SOLUTION

In stability analysis we use the method of normal modes (33, 34), whereby small disturbances are resolved into harmonic modes, which may be treated separately. Consider a typical wave component with

$$\zeta(\breve{z}, t) = Ae^{i(\omega t - k\breve{z})}, \quad \varphi_i(r, z, t) = R_i(r)e^{i(\omega t - kz)}, \quad i = g, l; \qquad [31]$$

$$V_j^l(r, z, t) = V_j(r)e^{i(\omega t - kz)}, \quad j = r, z;$$
$$p_i(r, z, t) = P_i(r)e^{i(\omega t - kz)}, \quad i = g, l. \qquad [32]$$

Here k is a real positive wave number. A mode with $\mathrm{Im}\omega < 0$ will be amplified, growing exponentially with time until it becomes so large that the nonlinear effects come to the forefront. If $\mathrm{Im}\omega = 0$, the mode is said to be neutrally stable, and if $\mathrm{Im}\omega > 0$, asymptotically stable or stable (33).

Equations [13], [14], and [22] with assumed t and z variations, Eqs. [31] and [32], are reduced to the system of Bessel equations

$$\frac{d^2R_i}{dr^2} + \frac{1}{r}\frac{dR_i}{dr} - k^2R_i = 0, \qquad [33]$$

$$\frac{d^2V_r}{dr^2} + \frac{1}{r}\frac{dV_r}{dr} - \alpha^2V_r - \frac{V_r}{r^2} = 0, \qquad [34]$$

$$\frac{d^2V_z}{dr^2} + \frac{1}{r}\frac{dV_z}{dr} - \alpha^2V_z = 0, \qquad [35]$$

where $\alpha^2 = (i\omega\rho_l/\eta_l) + k^2$.

The solution to the Bessel equations [33]–[35] has the following form:

$$R_i(r) = c_iI_0(kr) + d_iK_0(kr),$$
$$V_z(r) = a_lI_0(\alpha r) + b_lK_0(\alpha r),$$
$$V_r(r) = e_lI_1(\alpha r) + f_lK_1(\alpha r). \qquad [36]$$

Here, $I_n(z)$, $K_n(z)$ are the modified Bessel functions of order

n, and a_l, b_l, c_i, d_i, e_l, f_l are constants to be determined by the boundary conditions. Application of the boundary conditions [22], [24]–[30] leads to a system of four linear algebraic equations, which has a nontrivial solution provided that the determinant of the coefficients vanishes. The determinant represents the desired dispersion relation

$$D(\omega, k) = \begin{Vmatrix} I_1(kR_f) & I_1(\alpha R_f) & K_1(kR_f) & K_1(\alpha R_f) \\ kI_0(kR_f) & \alpha I_1(\alpha R_f) & -kK_0(kR_f) & -\alpha K_0(\alpha R_f) \\ 2k^2 I_1(kr_0) & (\alpha^2 + k^2) I_1(\alpha r_0) & 2k^2 K_1(kr_0) & (\alpha^2 + k^2) K_1(\alpha r_0) \\ d_{41} & d_{42} & d_{43} & d_{44} \end{Vmatrix} = 0. \quad [37]$$

Here,

$$d_{41} = -\frac{\omega^2 \rho_l I_0(kr_0)}{k} - \beta(\omega, k) I_1(kr_0) + i\eta_l \omega k (I_0(kr_0) + I_2(kr_0)),$$

$$d_{42} = -\beta(\omega, k) I_1(\alpha r_0) + i\eta_l \omega \alpha (I_0(\alpha r_0) + I_2(\alpha r_0)),$$

$$d_{43} = \frac{\omega^2 \rho_l K_0(kr_0)}{k} - \beta(\omega, k) K_1(kr_0) + i\eta_l \omega k (K_0(kr_0) + K_2(kr_0)),$$

$$d_{44} = -\beta(\omega, k) K_1(\alpha r_0) + i\eta_l \omega \alpha (K_0(\alpha r_0) + K_2(\alpha r_0)),$$

and

$$\beta(\omega, k) = \rho_g (\omega - kU)^2 \frac{K_0(kr_0)}{kK_1(kr_0)} + \left.\frac{\partial \Pi}{\partial h}\right|_{h=h_0} + \frac{\gamma}{r_0^2}(1 - (kr_0)^2).$$

If we set $\rho_g = 0$, $\Pi = 0$, $U = 0$, then Eq. [37] will coincide with Goren's dispersion relation for motionless fibers (16). Equation [37] is an implicit equation with respect to frequency, ω, that cannot be solved explicitly except for two limiting cases, the case of large Reynolds numbers and the case of highly viscous liquids. In this paper, the main effort focuses on understanding the large Reynolds number regime of flow.

V. NEGLIGIBLE VISCOSITY: THE KELVIN–HELMHOLTZ INSTABILITY

In this section we consider the inviscid approximation that implies the strong inequality $Uh_0\rho_l/\eta_l \gg 1$. The dispersion relation between the frequency and the wave number for an inviscid fluid can be derived from Eq. [37] considering the limit of vanishing η_l. However, it is easier to deal with the inviscid equations of motion directly. The two methods must yield the same results. We address this question below.

Considering the inviscid model, we have to designate $a_l = 0$, $b_l = 0$, $e_l = 0$, $f_l = 0$ in Eqs. [36]. Yielding all the resulting equations, we obtain the dispersion relation as

$$D_0(\omega, k) = (\omega - kU)^2 \rho_g \frac{K_0(kr_0)}{K_1(kr_0)} + \omega^2 \rho_l \frac{I_0(kr_0) K_1(kR_f) + I_1(kR_f) K_0(kr_0)}{I_1(kr_0) K_1(kR_f) - I_1(kR_f) K_1(kr_0)} - \frac{k\gamma}{r_0^2}\left((kr_0)^2 - 1 - \frac{r_0^2}{\gamma}\left.\frac{\partial \Pi}{\partial h}\right|_{h=h_0}\right) = 0. \quad [38]$$

The two first terms in the LHS of Eq. [38] are positive for any r_0, R_f. Indeed, the properties of the Bessel functions imply that because $r_0 > R_f$, for any wave number k, we have $I_1(kr_0) > I_1(kR_f)$ and $K_1(kr_0) < K_1(kR_f)$, and accordingly, $I_1(kr_0)/I_1(kR_f) > K_1(kr_0)/K_1(kR_f)$. The expression in the parentheses in the last term in the LHS of Eq. [38] is positive for stable films (see the stability condition [9]), which implies that the third term in the LHS of Eq. [38] is negative for some disjoining pressure isotherms and wave numbers corresponding to the adhesion hindered perturbations. Thus, Eq. [38] has at least one root, even in the case of a motionless fiber.

Motionless Fibers

For motionless fibers, $U = 0$, the solution of Eq. [38] corresponds to allowed capillary waves with the frequency

$$\omega_c = f_c(kr_0, kR_f, a)\left\{\frac{k\gamma}{\rho_l r_0^2}\left((kr_0)^2 - 1 - \frac{r_0^2}{\gamma}\left.\frac{\partial \Pi}{\partial h}\right|_{h=h_0}\right)\right\}^{1/2}. \quad [39]$$

The frequency depends on the thermodynamic dispersion relation, Eq. [9], and the hydrodynamic factor

$$f_c(kr_0, kR_f, a) = \left\{a\frac{K_0(kr_0)}{K_1(kr_0)} + \frac{I_0(kr_0) K_1(kr_0) + I_1(kR_f) K_0(kr_0)}{I_1(kr_0) K_1(kR_f) - I_1(kR_f) K_1(kr_0)}\right\}^{-1/2}, \quad [40]$$

where $a = \rho_g/\rho_l$ ($\ll 1$).

In the limiting case of ultrathin films, $h_0 \ll R_f$, Eq. [40] can be simplified. Taking into account the formula (35)

$$I_\mu(x)K'_\mu(x) - I'_\mu(x)K_\mu(x) = -1/x, \qquad [41]$$

with accuracy $O(a) + O(kh_0)^2$ one obtains

$$f_c(kr_0, kR_f, a) = \sqrt{kh_0} \qquad [42]$$

Thus, Eq. [42] has the same wave number dependence as that obtained in the lubrication approximation (26), yet the thickness-dependent factors differ. Below we address this point.

General Case

In a general case, $U \neq 0$, Eq. [38] is a quadratic equation; hence the number of roots depends on the sign of the discriminant

$$Di = \frac{k\gamma}{r_0^2}\left((kr_0)^2 - 1 - \frac{r_0^2}{\gamma}\frac{\partial\Pi}{\partial h}\bigg|_{h=h_0}\right)(C+D) - (kU)^2DC, \qquad [43]$$

where

$$C = \rho_g\frac{K_0(kr_0)}{K_1(kr_0)},$$

$$D = \rho_l\frac{I_0(kr_0)K_1(kR_f) + I_1(kR_f)K_0(kr_0)}{I_1(kr_0)K_1(kR_f) - I_1(kR_f)K_1(kr_0)}.$$

For stable modes, the discriminant Di must be positive. In the opposite case of the negative Di, Eq. [38] has two imaginary roots, $\omega_{1,2}$, one of which corresponds to the amplifying mode. The stability condition can be written in the dimensionless form

$$-(kr_0)^2 + \Delta + Wf_d(kr_0, R_f/r_0, a) < 0, \qquad [44]$$

where

$$f_d(kr_0, R_f/r_0, a) = kr_0(DC/\rho_g(C+D)) \qquad [45]$$

and

$$W = U^2\rho_g r_0/\gamma$$

is the Weber number; it measures the intensity of inertial forces relative to capillary ones.

Comparing with the stability condition for motionless fibers, inequality [9], we see that due to hydrodynamic interactions the third term in the LHS of the inequality [44] is always positive and plays a destabilizing role. This term is proportional to the Weber number. The dimensionless function $f_d(kr_0, R_f/r_0)$ depends exclusively upon geometry (fiber radius and film thickness) and inertial properties of fluids. When the ratio of densities is large, $a = \rho_g/\rho_l \ll 1$, the function $f_d(kr_0, R_f/r_0, a)$ becomes density independent. Thus, the stability condition for moving fibers depends on two dimensionless factors, the thermodynamic factor Δ and the hydrodynamic factor W. When the Weber number, W, vanishes, the stability condition [44] is reduced to the thermodynamic stability condition, Eq. [9].

Asymptotes

Because of the complexity of the function $f_d(kr_0, R_f/r_0, a)$, we cannot derive explicitly the stability condition. However, there are two limiting cases for which Eq. [38] can be solved explicitly.

1. Very short wave length, $\lambda \ll h_0 \ll r_0, R_f$; $kr_0 \gg 1$. In this case, the waves represent ripples on the film interface with wavelengths much smaller than the film thickness; parameters kR_f and kr_0 are large compared to unity. Using the asymptotic expressions (35) for the Bessel functions for $z \gg 1$, $I_\nu(z) \approx (e^z/\sqrt{2\pi z})$ and $K_\nu(z) \approx \sqrt{(\pi/2z)}e^{-z}$, the dispersion relation is reduced to the following form:

$$\rho_g(\omega - kU)^2 + \omega^2\rho_l\coth kh_0 = \frac{k\gamma}{r_0^2}((kr_0)^2 - \Delta). \qquad [46]$$

Equation [46] is similar to the known dispersion relation for shallow waves (36), where the parameter $-\Delta\gamma/r_0^2$ stands instead of gravity. For very short waves, $\lambda \ll h_0$, the dispersion relation [46] is reduced to the ordinary dispersion relation for capillary waves, or so-called Kelvin–Helmholtz waves (33, 34). A detailed analysis of the Kelvin–Helmholtz waves can be found in (36), see also (33), (34), (36). The stability condition is represented as the following inequality:

$$\frac{\rho_g U^2 r_0}{\gamma} \leq 2\sqrt{-\Delta}\,\frac{\rho_g + \rho_l}{\rho_l}. \qquad [47]$$

The critical wave number must exceed $1/h_0$,

$$k_{cr} = \frac{\sqrt{-\Delta}}{r_0} \gg \frac{1}{h_0}. \qquad [48]$$

In other words, the Kelvin–Helmholtz waves form only for quite stable films, actually, if the condition $\sqrt{-\Delta} \gg (r_0/h_0)$ is fulfilled. For van der Waals films the last condition is modified to $a_{HL}\sqrt{3} \gg h_0$. This is an upper estimate for the film thickness allowing the propagation of short waves. For organic fluids on dielectric fibers the modified Hamaker–Lifshitz constant is rather small, $a_{HL} \propto O$ (Å) (3, 8), so that the limit is not

realized. However, this limiting case is justified for helium films on quartz fibers, $a_{HL} \propto 10^{-7}$ cm (38).

2. Long waves, $h_0 \ll r_0$, $R_f \ll \lambda$; $kr_0 \ll 1$. Consider now the possibility of forming the waves with a length larger than the fiber radius. Using the asymptotic expansions (35) for the Bessel functions for $z \ll 1$, $K_0(z) \approx -\ln z$, $K_1(z) \approx z^{-1}$, $I_0(z) \approx 1$, $I_1(z) \approx z/2$, we can employ the following approximations:

$$\frac{K_0(kr_0)}{K_1(kr_0)} = -kr_0 \ln kr_0,\ I_0(kr_0)K_1(kR_f) \approx \frac{1}{kR_f},$$

$$I_1(kR_f)K_0(kr_0) \approx -\frac{kR_f}{2}\ln kr_0,$$

$$I_1(kR_f)K_1(kr_0) \approx \frac{R_f}{2r_0},$$

$$I_1(kr_0)K_1(kR_f) \approx \frac{r_0}{2R_f}.$$

Then, the second fraction in the LHS of the dispersion relation [38] is transformed into

$$\frac{I_0(kr_0)K_1(kR_f) + I_1(kR_f)K_0(kr_0)}{I_1(kr_0)K_1(kR_f) - I_1(kR_f)K_1(kr_0)} \approx \frac{2 - (kR_f)^2 \ln kr_0}{2kh_0},$$

and the dispersion relation [38] takes on the form

$$-(\omega - kU)^2 \rho_g kr_0 \ln kr_0 + \omega^2 \rho_l \frac{2 - (kr_0)^2 c^2 \ln kr_0}{2kh_0} = \frac{k\gamma}{r_0^2}((kr_0)^2 - \Delta), \quad [49]$$

where $c = R_f/r_0$. The discriminant of this quadratic equation has the form

$$Di = Wb\xi^2(2 - \xi^2 c^2 \ln \xi)\ln \xi - a\xi^2(\xi^2 - \Delta)\ln \xi + b(\xi^2 - \Delta)(2 - \xi^2 c^2 \ln \xi). \quad [50]$$

Here $\xi = kr_0$, $a = \rho_g/\rho_l$, and $b = r_0/2h_0$. Assuming that the ratio of densities is large, $a \ll 1$, we rewrite the discriminant as

$$Di = (W\xi^2 \ln \xi + \xi^2 - \Delta)(2 - \xi^2 c^2 \ln \xi)b. \quad [51]$$

The second cofactor in Eq. [51] is positive for any $\xi < 1$, i.e., within the range of validity of our approximations. Hence we have to determine a "positivity" condition for the first cofactor only. The critical condition $Di = 0$ is expressed as

$$-\ln \xi = \frac{1}{W}\left(\frac{-\Delta}{\xi^2} + 1\right). \quad [52]$$

The root of Eq. [52] first appears when the logarithmic branch in the LHS touches the hyperbolic branch in the RHS. The latter leads to the following system of equations:

$$\frac{1}{\xi} = \sqrt{\frac{W}{-2\Delta}} \gg 1, \quad [53]$$

$$\ln \frac{W}{-2\Delta} = 1 + \frac{2}{W}. \quad [54]$$

Inequality [53] means that the smaller the stability factor, the smaller the admissible Weber number. An asymptotic analysis of Eq. [54] can be done in terms of the variable $\theta = (2/W)$. Introducing the latter, Eq. [54] is rewritten in the form

$$\theta + \ln \theta = \lambda, \quad [55]$$

where $\lambda = -1 - \ln(-\Delta)$ is a large parameter. It can be proved that the solution to Eq. [55] has the asymptotic form (37)

$$\theta = \lambda\left[1 + \sum_{k=0}^{\infty}\sum_{m=1}^{\infty} \frac{c_{km}(\ln \lambda)^m}{\lambda^{k+m}}\right],$$

in which $c_{01} = -1$. Substituting this expression in the definition of θ, we obtain the asymptotic behavior of the limiting value of the Weber number, W, as a function of the thermodynamic factor, $\Delta(|\Delta| \ll 1)$:

$$W = \frac{2}{-\ln(-\Delta) - 1 - \ln(-1 - \ln(-\Delta))} + o\left(\frac{\ln(-1 - \ln(-\Delta))}{-\ln(-\Delta) - 1}\right). \quad [56]$$

It is noteworthy that even for very small absolute values of the thermodynamic factor the critical Weber numbers are appreciable. That is, the critical Weber number has a perceptible value of $W \approx 0.26$ when the thermodynamic factor is as small as $\Delta = -10^{-11}$. Consider for example organic liquid films on 10 μm fibers. The critical film thickness is estimated as $h_c \approx 0.1$ μm at $\gamma \approx 30$ dyne/cm (7, 8), and the thermodynamic factor $\Delta = -10^{-11}$ corresponds to the film thickness $h = h_c - 10^{-11}h_c/4$. These films become unstable when the fiber velocity exceeds the critical value $U = \sqrt{0.26\gamma/R_f\rho_g} \approx 10^3$ cm/s. Thus, the adhesion properties of fibers play a dominant role in the prevention of long wavelength instability in the high velocity spinning processes.

VI. THE EFFECTS OF VISCOSITY

In this section we consider a criterion of validity of the inviscid fluid approximation and discuss physical mechanisms of the film instability of thin films assuming that $h_0 \ll R_f$. In the subsection

on stability conditions, we derive viscosity-induced corrections to the stability criterion obtained in the inviscid fluid approximation (Eqs. [44], [45]). The subsection on characteristic times contains results on characteristic times of growth of unstable waves.

Consider the cases for which the modulus of the complex attenuation constant is smaller than the growth rate, i.e., when the diffusion time of propagation of vortices, $\tau_{\text{diffusion}} \approx \rho_l/k^2\eta_l$, is greater than the characteristic time of wave amplification. The latter can be roughly estimated from Eq. [39] as $\tau_{\text{wave}} \approx 1/\sqrt{-k\Delta\gamma/\rho_l r_0^2}$. For large Reynolds numbers and long waves the asymptotic equality $\tau_{\text{wave}} \approx r_0/U \ll \tau_{\text{diffusion}}$ holds, thus indicating that the inertial forces dominate the viscous ones. Hence, the attenuation constant can be calculated assuming that the velocity profile is similar to that for an inviscid fluid (see the Appendix). When the fiber velocity is small, $U \approx r_0/\tau_{\text{diffusion}}$, the viscous forces dominate the inertial ones and the inviscid model becomes ineligible.

Stability Conditions

Consider expansion of the dispersion equation [37] in powers of η_l. The inviscid approximation, Eq. [38], is the principal, viscosity-independent term in this expansion. We expect that for sufficiently large Reynolds numbers, $\text{Re} = Uh_0\rho_l/\eta_l$, a viscous correction to the critical frequency is small. Indeed, the first correction to Eq. [38] is

$$D_1(\omega, k) = \begin{Vmatrix} I_1(kR_f) & K_1(kR_f) \\ d_{41} & d_{43} \end{Vmatrix} = 0,$$

which can be represented as

$$D_1(\omega, k) = D_0(\omega, k) + 2i\eta_l\omega k^2 \times \frac{I_1(kR_f)K_1'(\xi) - K_1(kR_f)I_1'(\xi)}{K_1(kR_f)I_1(\xi) - I_1(kR_f)K_1(\xi)} = 0. \quad [57]$$

Let ω_0 be a root of $D_0(\omega, k) = 0$. For large Reynolds numbers we may take $\omega = \omega_0 + \delta$, where δ is a small attenuation constant. Then, δ is determined from

$$\delta \frac{\partial}{\partial\omega} D_0(\omega, k)\Big|_{\omega=\omega_0} \approx -2i\eta_l\omega_0 k^2 \frac{I_1(kR_f)K_1'(\xi) - K_1(kR_f)I_1'(\xi)}{K_1(kR_f)I_1(\xi) - I_1(kR_f)K_1(\xi)},$$

or

$$\delta \approx -2i\eta_l\omega_0^2 k^2 \frac{I_1(kR_f)K_1'(\xi) - K_1(kR_f)I_1'(\xi)}{K_1(kR_f)I_1(\xi) - I_1(kR_f)K_1(\xi)} \times \left(\omega_0 \left|\frac{\partial}{\partial\omega} D_0(\omega, k)\right|_{\omega=\omega_0}\right)^{-1}. \quad [58]$$

The numerator of Eq. [58] is positive due to the properties of the modified Bessel functions: functions $I_i(z)$ monotonically increase and their derivatives are positive; functions $K_i(z)$ monotonically decrease and their derivatives are negative. When the denominator is negative, the imaginary part of ε is negative for real ω_0, which leads to instability.

This fact provides another method for calculations of dangerous flow regimes. Solution of the dispersion relation [43] gives

$$\omega_0 = \frac{kUC}{C + D} \pm \frac{\sqrt{Di}}{C + D}, \quad [59]$$

where the discriminant, Di, and constants, C and D, are defined by Eq. [43]. Substituting Eq. [59] into denominator of Eq. [58], we obtain

$$\frac{\omega_0}{2}\frac{\partial}{\partial\omega} D_0(\omega, k)\Big|_{\omega=\omega_0} = \pm\omega_0 \times \sqrt{\frac{k\gamma}{r_0^2}\left((kr_0)^2 - 1 - \frac{r_0^2}{\gamma}\frac{\partial\Pi}{\partial h}\Big|_{h=h_0}\right)(C + D) - (kU)^2 DC}. \quad [60]$$

The sign in Eq. [60] corresponds to that taken in Eq. [59]. Thus, the denominator in Eq. [58] is negative when the frequency of the mode corresponding to the negative sign in Eq. [59] is positive. The relation for the critical wave number (or critical Weber number) is $\omega_0 = 0$ (negative branch); i.e.,

$$(k^*UC)^2 = Di^*.$$

Using the dimensionless variables, the latter takes the form

$$Wa\xi^2\left[\frac{K_0(\xi)}{K_1(\xi)}\right]^2 - \overline{Di}(\xi, a, W) = 0, \quad [61]$$

where we introduced the dimensionless discriminant as

$$\overline{Di}(\xi, a, W) = \frac{r_0^3}{\gamma\rho_l} Di.$$

After simple algebra, Eq. [61] is rewritten as

$$W = \frac{1}{\xi}(\xi^2 - \Delta)\frac{K_1(\xi)}{K_0(\xi)}. \quad [62]$$

The dangerous mode first appears just after the lower branch of

the solution [59] tangents the k-axis. This condition gives the following constraint:

$$Wa\,\frac{d}{d\xi}\left[\xi\,\frac{K_0(\xi)}{K_1(\xi)}\right]^2-\frac{d\overline{Di}(\xi,\,a,\,W)}{d\xi}=\frac{d}{d\xi}\left[W\xi\,\frac{K_0(\xi)}{K_1(\xi)}-(\xi^2-\Delta)\right]=0. \quad [63]$$

Note, neither the thermodynamic factor nor the Weber number depends upon the ratio of densities. Equations [62], [63] provide an explicit parameterized form of the $\Delta - W$ stability diagram (the parameter is the critical wave number).

Generally speaking, the critical conditions calculated by using Eqs. [62], [63] differ from those obtained by analyzing the roots of the discriminant (classical Kelvin–Helmholtz analysis). Actually, the presence of the first terms in the LHS of Eqs. [61] and [63] makes it possible to distinguish the Kelvin–Helmholtz instability from the discussed one. The difference is significant only if the complex Wa becomes of the order of unity or greater. For a reasonable velocity range, no more than $U = 10^4$ cm/s, this may be applicable for the "thick" fibers only. Indeed, the ratio of densities cannot vary in a broad range and, as a rule, fluctuates around 10^{-3}. Due to their small surface energy, the apolar liquids have more chances to undergo the Kelvin–Helmholtz instability than the polar ones. Therefore, underestimating the surface tension by the value $\gamma \approx 10$ dyne/cm one gets that the fiber radius should be 1 cm or greater. But the associated Reynolds number falls into the range of turbulence, so that the model becomes inapplicable for such thick fibers. At the same time, the difference between the criteria for the Kelvin–Helmholtz instability and those for the "viscosity induced" instability could be significant near the phase transition where both phases have almost the same density and the surface tension is very small. *Thus, the instability may arise for the gas velocities smaller than the critical velocity of the Kelvin–Helmholtz instability* discussed in Section V.

Taking into account formula [41] and eliminating the Weber number in Eq. [63], the critical thermodynamic factor can be represented in leading order as

$$\Delta=-\frac{\xi^2}{2}\left(\frac{K_1^2(\xi)}{K_0^2(\xi)}-1\right)\left(\frac{1}{2}-\frac{1}{2}\,\frac{K_1^2(\xi)}{K_0^2(\xi)}+\frac{K_1(\xi)}{\xi K_0(\xi)}\right)^{-1}. \quad [64]$$

Equations [62]–[64] allow us to eliminate the wave number and plot a stability diagram in terms of the thermodynamic stability factor, Δ, and Weber number, W (Fig. 2).

For thin van der Waals films, $h_0 \ll R_f$, we arrive at the relation between the critical film thickness and the critical wave number

$$h_c^W = h_c\varepsilon(W) = 3^{1/4}\sqrt{a_{HL}R_f}\,\varepsilon(W), \quad [65]$$

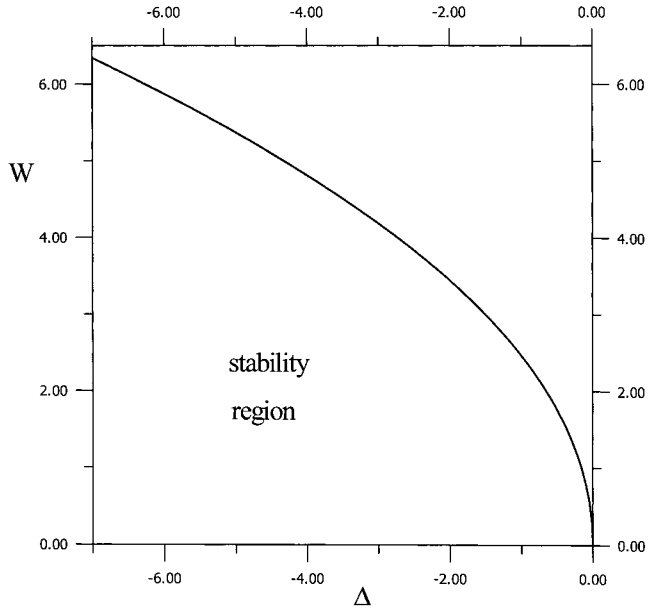

FIG. 2. Stability diagram.

where $\varepsilon = (1 - \Delta)^{-1/4}$, and the thermodynamic factor, Δ, is defined by Eq. [64]. For motionless fibers, Eq. [65] reduces to the critical film thickness of thermodynamically stable films (7); see Section II.

To resume, there are two types of unstable modes: the first corresponds to the Kelvin–Helmholtz waves with the negative imaginary part of ω_0, while the second type constitutes the waves with the zeroth imaginary part of ω_0 and with the negative imaginary part of the viscous correction. The second type of waves are transformed into the Kelvin–Helmholtz waves of the first type when the two branches of Eq. [59] intersect. The Kelvin–Helmholtz instability is affected by the ratio of fluid densities, while the viscosity-induced instability is not.

Characteristic Times

Consider the characteristic break-up time of unstable modes. The characteristic growth rate (or break-up time T) can be represented as

$$\frac{1}{T}=\frac{1}{\tau}-\frac{1}{\tau_\eta}, \quad \text{for the Kelvin-Helmholtz waves,} \quad [66]$$

$$\frac{1}{T}=\frac{1}{\tau_\eta}, \quad \text{for the viscosity-induced waves.} \quad [67]$$

Here, τ is the modulus of the imaginary part of Eq. [59], and τ_η is the modulus of Eq. [58] in which only the imaginary part of ω_0 is retained. One can see that the fluid viscosity is a stabilizing factor for the Kelvin–Helmholtz waves, and a destabilizing one for waves of the second type. As shown in the

Appendix, the denominator of Eq. [58] is the wave or excess energy, consisting of the potential energy caused by the capillary and surface forces, as well as of the kinetic energy of moving perturbations. The excess energy becomes negative when the wave excitation lowers the total energy of the unperturbed moving system (Pierce (40), Bendjamin (41), Cairns (42), Stepanyants and Fabrikant (37)). In the case under consideration, the energy becomes negative whenever the film thickness oscillations are in phase with the flow velocity oscillations. An interpretation of the physical mechanism of "viscous" destabilization is given in the Appendix.

Under practical conditions of film coating, the film thickness may be inconsistent with its value in thermodynamic equilibrium. That is, the film is basically unstable even for motionless fibers. Thus, the Kelvin–Helmholtz instability is more important for technological applications, and we turn our attention to this class.

Consider some properties of the Kelvin–Helmholtz waves. First, let's find a criterion of dynamic stability of thin films. Comparing the modulus of ω_0 and δ, we see that our theory is applicable if and only if the inequality $\tau/\tau_\eta \ll 1$ holds. Otherwise, the viscous forces dominate the inertial ones and the film stability is expected. The wave number k_* of the fastest growing mode corresponds to the maximum of the imaginary part of ω_0 with respect to the wave number k. This maximum always exists because the interval of wave numbers admissible for instability has an upper boundary equaled to the critical wave number. For larger wave numbers (smaller wavelengths), the capillary forces suppress the excitations. Using that the parameter $(1 - c)/c = h_0/R_f$ is small and accounting for Eq. [41], the characteristic break-up time can be written from Eq. [59] as

$$\tau = f_\tau(W, \Delta)\sqrt{R_f r_0^3 \rho_l/\gamma h_0}, \qquad [68]$$

where

$$f_\tau(W, \Delta) = \left\{\xi_f\sqrt{-(\xi_f^2 - \Delta) + \frac{(-2\xi_f^2 + \Delta)}{u}\frac{K_0(\xi_f)}{K_1(\xi_f)}}\right\}^{-1}, \qquad [69]$$

and

$$u = -2\frac{K_0(\xi_f)}{K_1(\xi_f)} + \frac{\xi_f}{2} - \frac{\xi_f}{2}\left(\frac{K_0(\xi_f)}{K_1(\xi_f)}\right)^2. \qquad [70]$$

In Eqs. [68]–[70], ξ_f is the critical dimensionless wave number of the fastest growing mode. The ξ_f is a positive solution of the equation

$$W = (-2\xi_f^2 + \Delta)/u\xi_f. \qquad [71]$$

Invoking asymptotic properties of the modified Bessel functions and taking into account that the function $K_0(\xi)/K_1(\xi)$ is monotone, one obtains that u, Eq. [70], varies monotonically from zero to $-3/2$. Therefore, a positive solution to Eq. [71] exists in the interval $\xi_f \in [\sqrt{\Delta/2}, \infty)$. Hence, if the fiber is motionless, the fastest growing mode corresponds to the wave number $\sqrt{\Delta/2}$ (this conclusion also follows from Eqs. [39], [42]). If the film is so thick that the disjoining pressure can be neglected ($\Delta = 1$) yet the inequality $h_0 \ll R_f$ holds, the critical wave number is $\xi_f = \sqrt{1/2} = 0.707$ (see also Eqs. [39], [42]). It is a little bit greater than Rayleigh's capillary mode for jets, $\xi_{\text{Rayleigh}} = 0.697$ (Rayleigh (27)). The greatest value of the dimensionless break-up time is $f_\tau(0, 1) = 2$.

Thus, for thin films $h_0 \ll R_f$, the time of ripple growth is inversely proportional to the square root of the film thickness, yet it is implicitly affected by the film thickness via the thermodynamic factor. Assuming for a moment $f_\tau \approx O(1)$ (motionless fibers), $\gamma = 30$ dyne/cm, $R_f = 10\ \mu$, and $\rho_l = 1$ g/cm^3, one obtains an estimate for the characteristic break-up time as $\tau \approx \sqrt{R_f/h_0} \times 10^{-5}$ s.

In the same case, $h_0 \ll R_f$, the characteristic time of wave damping caused by viscous forces is estimated as

$$\tau_\eta = \chi(W, \Delta)\frac{\rho_l r_0^2}{\eta_l} = \frac{R_f \rho_l r_0^2}{h_0 \eta_l \xi_f^3}. \qquad [72]$$

Thus, in the limiting case $h_0 \ll R_f$, the time of viscous damping depends on the film thickness as $\tau_\eta \propto R_f/h_0$ and via the thermodynamic factor as well. This dependence differs significantly from the expected reverse cubic law of Boussinesq and Reynolds due to a different physical situation. In the ordinary lubrication theory one suggests that the film fluid works out the Poiseuilleian profile to satisfy the no-slip and no-stress boundary conditions at the fiber surface and the liquid–gas interface, respectively. But for large Reynolds numbers the physical scheme of fluid flow is akin to that observed at the sudden stretching of a nylon stocking. Almost all the particles have the same velocity and only a very small transition layer forms a Poiseuilleian profile. In our case the stretching force is the compressing hydraulic head, $F_{\text{extension}} \approx 2\pi R_f \rho_l U^2 \lambda$, driving the film to extend. Because of viscosity, the liquid film resists stretching with the force $F_{\text{friction}} \approx 2\pi R_f h_0 \eta_l U/R_f$. Accounting for both forces and assuming $U \approx R_f/\tau_\eta$, $\lambda \approx R_f$, one gets the dimensional factor in Eq. [72]. For $\xi_f \propto O(1)$, $R_f = 10\ \mu$, $\rho_l = 1$ g/cm^3, and $\eta = 10^{-2}$ ps, we obtain the estimate $\tau_\eta \approx R_f/h_0 \times 10^{-4}$ s. The estimate shows that the inequality $\tau/\tau_\eta \ll 1$ holds for any water films with reasonable thickness; i.e., they are unstable.

It should be noted that Eq. [72] holds true for the viscosity-induced waves as well, provided that ξ_f lies in the allowed range specified by the inequalities $0 < \omega_0^-(\xi_f, W, \Delta) < \omega_0^+(\xi_f, W, \Delta)$, where the plus and minus subscripts denote the corresponding branches of Eq. [59].

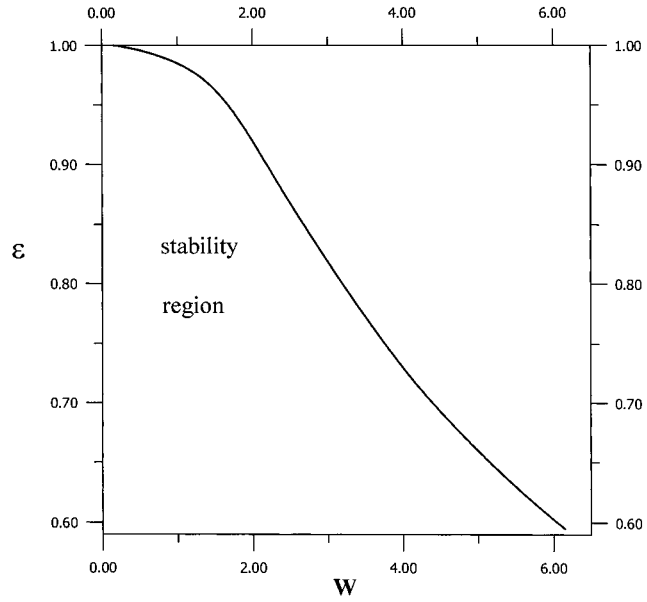

FIG. 3. The correction factor ε as a function of the Weber number W.

VII. NUMERICAL RESULTS AND DISCUSSION

Analyses of the stability diagram can be done numerically. Fortunately, when the ratio of densities is large, $a \ll 1$, the solutions of Eqs. [62] and [52] are practically indistinguishable for long waves. For short waves, asymptotic analysis of Eqs. [62], [63] for any ratio of densities can be found elsewhere (36), (37). However, when $a \ll 1$, the solution coincides with Eq. [47] with accuracy $O(a)$. Therefore, numerical analyses may be performed in a finite range of wave numbers and then analytically continued by asymptotes. A numerical solution of Eqs. [62], [63] is plotted in Figs. 2 and 3. On moving fibers, the thermodynamically unstable films characterized by the positive factor Δ (inequality [9]) remain unstable. The liquid–air interactions enhance interfacial fluctuations and can drive the thermodynamically stable films, characterized by the negative factor Δ, to the edge of stability. The line $W_c(\Delta)$ divides the plane of parameters into two regions, the stable region below and the unstable region above. $W_c(\Delta)$ gives the critical value of the Weber number that corresponds to the appearance of hydrodynamic instability in the primarily stable films. As Δ approaches zero, $W_c(\Delta)$ diminishes.

For the van der Waals films, the thermodynamic factor Δ varies from 1, for sufficiently thick films whose behavior is governed predominantly by the destabilizing action of capillarity, to negative values corresponding to the thermodynamically stable films. We analyzed how the hydrodynamic interactions affected the stability conditions for the van der Waals films. In Fig. 3, the correction factor ε, Eq. [65], is plotted as a function of the Weber number. The critical thickness of thermodynamically stable films on motionless fibers was estimated in Section II, and it corresponds to $W = 0$. As W increases the critical thickness decreases, which reflects the enhancement of interface disturbances due to the film–air interaction. The reduction of the critical film thickness may be significant. For example, assuming typical values for parameters, $a_{HL} \approx 1$ Å, $R_f \approx 10$ μ, $\gamma \approx 30$ dyne/cm, we obtain that the critical thickness for motionless fibers is $h_c \approx 42$ nm, while the critical thickness reduces to $h_c \approx 27$ nm when the fiber speed becomes $U \approx 10^4$ cm/s.

The condition of thermodynamic stability shows that the least critical wave number is the zeroth one; i.e., the film as a whole loses its uniformity as the thermodynamic factor Δ approaches zero, Eq. [9]. In contrast, the critical conditions of hydrodynamic stability imply that the critical wavelength and, correspondingly, the critical wave number are finite (Fig. 4). At the same time, the break-up time of the critical mode is infinite. In other words, there is a barrier in wavelengths of stable periodic undulations that separates dynamically stable undulations from unstable ones. The competition among the imposed pressure head, capillary pressure, and adhesion properties of fibers selects allowed modes.

The break-up time of unstable films is also affected by the fluid–solid interactions expressed in terms of a disjoining pressure isotherm. However, since the growth of instability begins just after the film is deposited, we can put for estimate $\Delta = 1$. The latter implies that the disjoining pressure can be ignored for initial instants of time. In Figs. 5 and 6 we plot the characteristic time of wave amplification and the characteristic time of wave damping in dimensionless form. Using these diagrams, we can assess the critical film thickness as $\sqrt{h_0/R_f} = U_{cap}\chi(W, 1)/U_{vis}\, f_\tau(W, 1)$, where $U_{cap} = \sqrt{\gamma/\rho_l R_f}$ is the characteristic velocity of capillary waves and $U_{vis} = \eta_l/\rho_l R_f$ is the characteristic velocity of propagation of disturbances in viscous fluids. If the film thickness is larger than this value, the apparent velocity of capillary waves is greater, and the film breaks down. And vice versa, for thin films the viscous forces

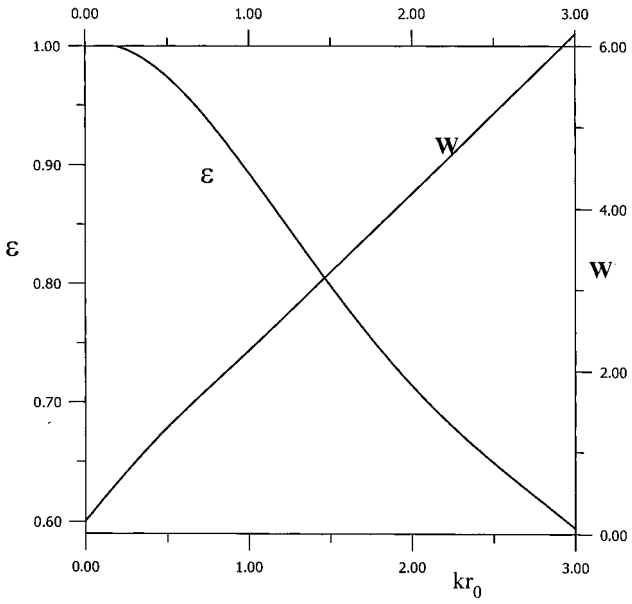

FIG. 4. The correction factor ε and the critical Weber number W_c as functions of the dimensionless wave number.

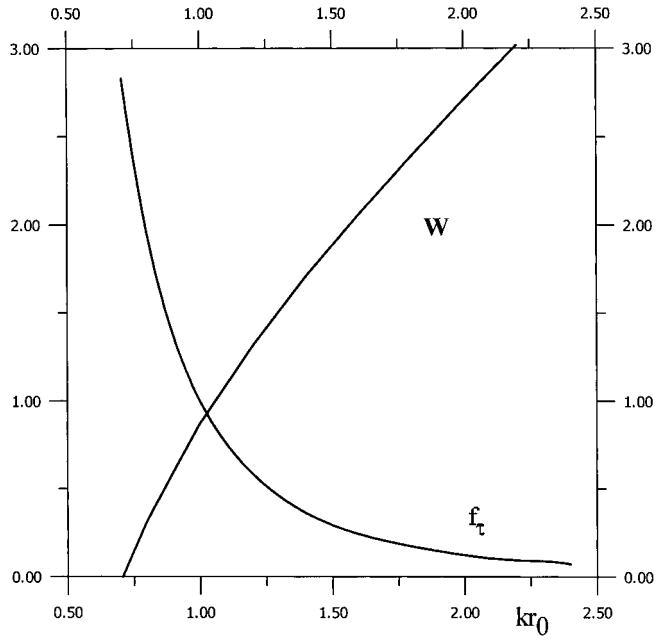

FIG. 5. "Inertial" time and Weber number as functions of the critical wave number.

dominate the others and stabilize the interface. Accounting for typical physical parameters, we see that the viscous damping is important only for short waves, while the large drops grow practically nondamped. Due to the difference in physical causes of instabilities, the lubrication approximation predicts that the characteristic time is inversely proportional to film thickness *cubed*, $\tau_\eta \propto 1/h_0^3$ (Yarin *et al.* (25), Chen and Hwang (26)), while in the discussed regime the time is inversely proportional to film thickness $\tau_\eta \propto 1/h_0$. Thus, the characteristic flow regimes can be distinguished by measuring the break-up time and film thickness.

VIII. CONCLUSIONS

The stability of liquid films on moving fibers has been analyzed with a focus on effects caused by film–solid adhesion interactions and hydrodynamic interactions between the film and surrounding gas. We have shown that at high fiber velocities the film–gas hydrodynamic interactions induce instability in the films, which would be stabilized by the adhesion interactions at static conditions. This effect, specific for moving fibers, has been named the wind effect. The wind effect may lead to film destruction and droplet formation, which are negative factors in various technologies related to fabrication and chemical modification of fibers and fiber products, e.g., spin finishing and lubrication.

The film–fiber adhesion interactions are expressed in terms of the thickness-dependent disjoining pressure, which controls conditions of thermodynamic equilibrium on motionless fibers and determines the adhesion factor of thermodynamic stability, Δ. The adhesion factor, Δ, implies the upper limit of stable film thicknesses and wave lengths of dangerous perturbations for a given liquid surface tension and fiber diameter. In the case of moving fibers, the hydrodynamic effects enhance the interfacial instabilities and impose more severe conditions of film stability. When the initial film is thermodynamically unstable ($\Delta > 0$), hydrodynamic flow affects the growth rate and critical wavelength. When the initial film is thermodynamically stable ($\Delta < 0$), two types of unstable modes are shown to be caused by hydrodynamic factors: the first corresponds to the Kelvin–Helmholtz waves induced by inertia effects; the second, induced by viscosity effects, is observed at smaller (yet still large) Reynolds numbers when the Kelvin–Helmholtz instability is suppressed.

The magnitude of film–gas hydrodynamic interactions is quantified by the Weber number, *W*, that measures the intensity of inertial forces relative to capillary forces. As the Weber number increases the critical thickness of stable films decreases and the characteristic break-up time for unstable films reduces substantially. We have demonstrated that the allowed Weber numbers may be large if and only if the negative adhesion factor is large. In this case, the instability looks like a ripple formation. If the negative adhesion factor is small, the resulting instability leads to the formation of drops of characteristic size on the order of the fiber radius. We have derived conditions of film stability and analyzed the unstable modes in terms of two dimensionless parameters, the adhesion factor, Δ, and the Weber number, *W*. The Reynolds number, Re, determines the regions of validity of different approximations.

Linear stability analysis of the system of coupled hydrodynamic equations of film and gas flow has been performed by the method of normal modes. We derived the general dispersion relation as an implicit equation with respect to the mode frequency. In the limit of vanishing fiber velocities, the obtained equation provides the dispersion equation for motionless fibers.

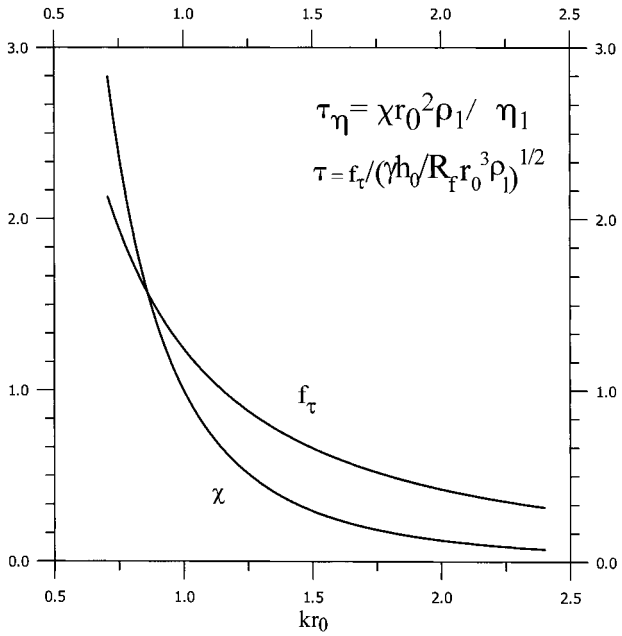

FIG. 6. "Inertial" and "viscous" times as functions of the critical wave number.

This equation represents a generalization of the dispersion relation derived by Goren (16), in which the disjoining pressure effects were not considered.

In the large Reynolds number regime, the obtained general dispersion relation is expanded in the power series of inverse Reynolds numbers, and is solved in the first order. The principal term of the series corresponds to the inviscid approximation. The explicit forms of the dispersion relation have been derived in two limiting cases of very short (much smaller than the film thickness) and very long (much larger than the fiber radius) wavelengths. In the inviscid approximation, the film instability is similar to the Kelvin–Helmholtz mechanism of formation of capillary waves.

The first correction reflects viscosity effects in the growth rate of unstable modes. Viscosity effects are essential for velocities smaller than the critical velocity of the Kelvin–Helmholtz instability obtained in the inviscid approximation. Increasing the fiber velocity, we first encounter the film instability caused by coherence in oscillations of film thickness and flow velocity. Connected via the no-slip boundary condition, viscous and potential components of velocity thus transfer the kinetic energy of moving fiber into the potential and kinetic energy of the interface. Thus, the fluid viscosity plays here a critical role.

For thin films, with thickness much less than the fiber radius, we have obtained the explicit formulas for the borders of stability expressed via the adhesion factor, Weber number, and critical wavelength. For the van der Waals films, the critical thickness is represented as a product of its thermodynamic value, characteristic for motionless fibers, and a correction factor, which depends upon the Weber number. The growth rates of the fastest growing modes are estimated for both types of unstable modes. In contrast to the lubrication approximation, in which the break-up time is inversely proportional to the film thickness cubed (26), we have found that the break-up time is inversely proportional to the square root of thickness with a multiplier, which implicitly depends on the film thickness through the adhesion factor. The damping time is found to be inversely proportional to the film thickness with a multiplier, which also implicitly depends on the film thickness through the adhesion factor.

When disjoining pressure is negligibly small and the fiber is motionless, the critical wave number is slightly greater than the Rayleigh criterion for jet stability.

The results are illustrated by the estimates of the stability conditions for moving fibers in terms of the stability diagram, the critical film thickness, the fastest unstable mode, and the corresponding characteristic break-up time. The estimates were done for practical conditions of fiber processing. Although the methods developed are applicable to any type of liquid–solid interaction, practical estimates were made for the long-range van der Waals interactions, which likely dominate the film–fiber interactions in many practical situations.

ACKNOWLEDGMENT

This work was supported by a group of TRI corporate participants.

APPENDIX

To elucidate formula [58], it is convenient to consider the procedure of direct calculation of the attenuation constant $\mathcal{T}\delta$ used by Landau and Lifshitz (34). Recall that the attenuation constant $\mathcal{T}\delta$ is defined as

$$\mathcal{T}\delta = -\frac{\langle \dot{S} \rangle}{2\langle E \rangle}, \qquad \text{[A1]}$$

where $\langle \dot{S} \rangle$ is the rate of energy dissipation due to internal friction in the fluid and $\langle E \rangle$ is the wave energy. The angle brackets denote an average over the oscillations. Below, the time-Fourier images have the same denotations as corresponding functions in the main text. Formula [A1] reads that the wave energy decreases with time exponentially, and the cofactor 2 accounts for the fact that the energy is proportional to the squared amplitude. The rate of energy dissipation for a viscous fluid can be written as

$$\langle \dot{S} \rangle = -4\pi\eta_l \int \left(\frac{\partial \nu_i^l}{\partial x_k} \right)^2 r dr dz, \qquad \text{[A2]}$$

and the wave energy is represented as a sum of kinetic and potential energies of the system. The kinetic energy is

$$\langle T \rangle = \frac{\rho_g}{2} \int dz \int_{r_0+\zeta}^{\infty} \left\{ \left(U + \frac{\partial \varphi_g}{\partial z} \right)^2 - U^2 + \left(\frac{\partial \varphi_l}{\partial r} \right)^2 \right\} 2\pi r dr + \frac{\rho_l}{2} \int dz \int_{R_f}^{r_0+\zeta} \left\{ \left(\frac{\partial \varphi_l}{\partial z} \right)^2 + \left(\frac{\partial \varphi_l}{\partial r} \right)^2 \right\} 2\pi r dr. \qquad \text{[A3]}$$

The kinetic energy to second order in the velocity potentials and surface displacement is rewritten as

$$\langle T \rangle \approx \frac{\rho_g}{2} \int dz \int_{r_0}^{\infty} \left\{ \left(\frac{\partial \varphi_g}{\partial z} \right)^2 + \left(\frac{\partial \varphi_l}{\partial r} \right)^2 \right\} 2\pi r dr - \frac{\rho_g}{2} \int dz 2U \frac{\partial \varphi_g}{\partial z} \zeta \Big|_{r_0} 2\pi r_0 + \frac{\rho_l}{2} \int dz \int_{R_f}^{r_0} \left\{ \left(\frac{\partial \varphi_l}{\partial z} \right)^2 + \left(\frac{\partial \varphi_l}{\partial r} \right)^2 \right\} 2\pi r dr. \qquad \text{[A4]}$$

Note that in the first and third terms of Eq. [A4], integrating by parts, the integrals can eliminate z-derivatives. Integrating the remaining parts over the r-coordinate and using the boundary condition at the fiber, we can reduce the first and third integrals to the integrals over the unperturbed gas–liquid interface. Re-

call that the r-dependent parts of the velocity potentials are represented as, in the upper region,

$$R_g(r) = d_g K_0(kr), \quad d_g = -\frac{iA(\omega - kU)}{kK_1(kr_0)} \qquad [A5]$$

and, in the film region,

$$R_l(r) = c_l(I_0(kr) + d_l K_0(kr)), \quad d_l = \frac{I_1(kR_f)}{K_1(kR_f)},$$

$$c_l = \frac{iA\omega}{k\left(I_1(kr_0) - \dfrac{I_1(kR_f)}{K_1(kR_f)} K_1(kr_0)\right)}. \qquad [A6]$$

Then the contribution due to kinetic energy is, to second order in wave amplitude and averaged over the oscillations,

$$\langle T\rangle = \frac{\pi\rho_g r_0}{2k}\frac{K_0(kr_0)}{K_1(kr_0)}((\omega - kU)^2 + 2kU(\omega - kU))A^2 + \frac{\pi\omega^2\rho_l r_0}{2k}\frac{I_0(kr_0)K_1(kR) + I_1(kR)K_0(kr_0)}{I_1(kr_0)K_1(kR) - I_1(kR)K_1(kr_0)}A^2. \qquad [A7]$$

The potential energy of each wave equals the work against the capillary and surface forces. The work is calculated, accounting for Eq. [8], as

$$\langle H\rangle = -\pi r_0 \int \left\{\left.\frac{\partial\Pi}{\partial h}\right|_{h=h_0} + \gamma\left(\frac{1}{r_0^2} - k^2\right)\right\}A^2\cos^2(kz - \omega t)dz. \qquad [A8]$$

Using the fact that the waves satisfy the dispersion relation [58], we obtain the energy in the form

$$\begin{aligned}\langle E\rangle &= \langle T\rangle + \langle H\rangle \\ &= \frac{\pi\rho_g r_0}{k}\frac{K_0(kr_0)}{K_1(kr_0)}((\omega - kU)^2 + kU(\omega - kU))A^2 \\ &\quad + \frac{\pi\omega^2\rho_l r_0}{k}\frac{I_0(kr_0)K_1(kR_f) + I_1(kR_f)K_0(kr_0)}{I_1(kr_0)K_1(kR_f) - I_1(kR_f)K_1(kr_0)}A^2 \\ &= \left\{\frac{\pi\rho_g r_0}{k}\frac{K_0(kr_0)}{K_1(kr_0)}(\omega - kU) \right. \\ &\quad \left. + \frac{\pi\omega\rho_l r_0}{k}\frac{I_0(kr_0)K_1(kR_f) + I_1(kR_f)K_0(kr_0)}{I_1(kr_0)K_1(kR_f) - I_1(kR_f)K_1(kr_0)}\right\}\omega A^2 \\ &= \frac{\pi r_0\omega}{2k}\frac{\partial}{\partial\omega}D_0(\omega, k)A^2. \end{aligned} \qquad [A9]$$

Substituting into Eq. [A2] the velocity field in the inviscid fluid approximation, Eqs. [A5], [A6], we can write the dissipation rate as

$$\begin{aligned}\langle\dot{S}\rangle &= -2\pi\eta_l r_0 R_l'(r_0)R_l''(r_0) \\ &= -2\pi\eta_l r_0\omega^2 k\frac{K_1(kR_f)I_1'(\xi) - I_1(kR_f)K_1'(\xi)}{K_1(kR_f)I_1(\xi) - I_1(kR_f)K_1(\xi)}A^2. \end{aligned} \qquad [A10]$$

Substituting Eqs. [A9] and [A10] into definition [A1], we arrive at the same result, Eq. [58]. One can see that the denominator is the wave energy, which becomes negative when the wave excitation lowers the total energy of the unperturbed moving system (Pierce (40), Bendjamin (41), Cairns (42), Stepanyants and Fabrikant (37)). The concept of the negative energy provides a good method for calculating the dangerous flow regimes. In recent years, the effect of "viscous" destabilization has been much discussed in different contexts (37).

REFERENCES

1. Kheifets, L. I., and Neimark, A. V., "Multiphase Processes in Porous Media." Khimia, Moscow, 1982.
2. Derjaguin, B. V., and Churaev, N. V., "Wetting Films." Nauka, Moscow, 1984.
3. Derjaguin, B. V., Churaev, N. V., and Muller, V. M., "Surface Forces." Plenum, New York, 1987.
4. White, D. A., and Tallmadge, J. A., *J. Fluid Mech.* **23,** 325 (1965).
5. Carroll, B. J., *J. Colloid Interface Sci.* **57,** 488 (1976).
6. Starov, V. M., and Churaev, N. V., *Colloid. J. USSR* **40,** 909 (1978).
7. Brochard-Wyart, F., *C. R. Acad. Sc. Paris Ser. II* **303,** 1077 (1986).
8. Brochard, F., *J. Chem. Phys.* **84,** 4664 (1986).
9. Carroll, B. J., *Langmuir* **2,** 248 (1986).
10. Quere, D., Du Miglio, J.-M., and Brochard-Wyart, F., *Rev. Phys. Appl.* **23,** 1023 (1988).
11. Bacri, J. C., Frenois, C., Perzynski, R., and Salin, D., *Rev. Phys. Appl.* **23,** 1017 (1988).
12. Quere, D., Du Miglio, J.-M., and Brochard-Wyart, F., *Europhys. Lett.* **10,** 335 (1989).
13. Novakovski, B., and Rukenstein, E., *J. Colloid Interface Sci.* **148,** 249 (1992).
14. McHale, G., Kab, N. A., Newton, M. I., and Rowan, S. M., *J. Colloid Interface Sci.* **186,** 453 (1997).
15. Bruyn de, J. R., *Phys. Fluids* **9,** 1599 (1997).
16. Goren, S. L., *J. Fluid Mech.* **12,** 309 (1962).
17. Hasegawa, E., and Nakaya, C., *J. Phys. Soc. Jpn.* **29,** 1634 (1970).
18. Dumbleton, J. H., and Hermans, J. J., *Ind. Eng. Chem. Fund.* **9,** 466 (1970).
19. Lin, S. P., and Liu, W. C., *AIChE J.* **21,** 775 (1975).
20. Krantz, W. B., and Zollars, R. L., *AIChE J.* **22,** 930 (1976).
21. Tougou, H., *Phys. Soc. Jpn.* **43,** 318 (1977).
22. Solorio, F. J., and Sen, M., *J. Fluid. Mech.* **183,** 365 (1987).
23. Johnson, M., Kamm, R. D., Ho, L. W., Shapiro, A., and Pec, T. J., *J. Fluid Mech.* **233,** 141 (1991).
24. Cheng, M., and Chang, H.-C., *Chem. Eng. Commun.* **118,** 327 (1992).
25. Yarin, A. L., Oron, A., and Roseneau, P., *Phys. Fluids A* **5,** 91 (1993).
26. Chen, J. L., and Hwang, C. C., *J. Colloid Interface Sci.* **182,** 564 (1996).
27. Rayleigh, L., *Proc. Roy. Soc. A* **29,** 71 (1879); *Phil. Mag.* **34,** 145 (1892).
28. Derjaguin, B. V., *Acta Phys. Chim. URSS* **12,** 181 (1940).

29. Derjaguin, B. V., *J. Colloid Interface Sci.* **49,** 249 (1974).
30. Neimark, A. V., *J. Adhesion Sci. Technol.*, **17** (1999).
31. Walcsak, Z. K., "Formation of Synthetic Fibers." Gordon and Breach, New York, 1977.
32. Plateau, J., "Statique Experimentale et Théorique des Liquides Soumis aux Seules Forces Moléculaires." Gauthier–Villars, Paris, 1873.
33. Drazin, P. G., and Reid, W. H., "Hydrodynamic stability." Pergamon, Oxford, 1981.
34. Landau, L. D., and Lifshitz, E. M., "Hydrodynamics." Nauka, Moscow, 1986.
35. Abramowitz, M., and Stegan, I. A., Eds., "Handbook of Mathematical Functions." Dover, New York, 1965.
36. Lamb, H., "Hydrodynamics," 6th ed. Cambridge University Press, Cambridge, UK, 1932, Dover, New York, 1945.
37. Stepanyants, Yu. A., and Fabrikant, A. L., *Sov. Phys. Uspekhi* **159,** 83 (1989); "Propagation of Waves in Shear Flows." Nauka, Moscow, 1996.
38. Sabisky, E. S., and Anderson, C. H., *Phys. Rev. Lett.* **30,** 1122 (1973); *Phys. Rev. A* **7,** 790 (1973).
39. Fedoryuk, M. V., "Asymptotics: Integrals and Series." Nauka, Moscow, 1987.
40. Pierce, J., "Almost All about Waves." MIT Press, London, 1974.
41. Bendjamin, T. B., *J. Fluid Mech.* **16,** 436 (1963).
42. Cairns, R. A., *J. Fluid Mech.* **92,** 1 (1979).